[6]Forte, I., and Shinar, J., "Improved Guidance Law Design Based on the Mixed-Strategy Concept," *Journal of Guidance, Control, and Dynamics*, Vol. 12, No. 5, 1989, pp. 739–745.

[7]Ben-Asher, J., and Yaesh, I., *Advances in Missile Guidance Theory*, Vol. 180, Progress in Astronautics and Aeronautics, AIAA, Washington, DC, 1998, Chap. 5.

[8]Deshpande, J. G., Upadhay, T. N., and Lainiotis, D. G., "Adaptive Control of Linear Stochastic Systems," *Automatica*, Vol. 9, 1973, pp. 107–115.

[9]Maybeck, P. S., *Stochastic Models, Estimation and Control*, Vol. 3, Academic, New York, 1984, pp. 247–257.

[10]Stepaniak, M. J., and Maybeck, P. S., "MMAE-Based Control Redistribution Applied to the VISTA F-16," *IEEE Transactions on Aerospace and Electronic Systems*, Vol. 34, No. 4, 1998, pp. 1249–1260.

[11]Maybeck, P. S., and Stevens, R. D., "Reconfigurable Flight Control via Multiple Model Adaptive Control Methods," *IEEE Transactions on Aerospace and Electronic Systems*, Vol. 27, No. 4, May 1991, pp. 470–480.

Class of Rotations Induced by Spherical Polygons

Ranjan Mukherjee* and Jay T. Pukrushpan†
Michigan State University,
East Lansing, Michigan 48824-1226

Introduction

THE geometry of rotations is critical to the analysis of diverse problems ranging from the motion of celestial bodies to the dexterous manipulation of objects subject to nonholonomic constraints. In a number of these problems, the use of orientation coordinates such as Euler angles[1] and Euler parameters[1] becomes necessary since angular velocities are nonintegrable in nature.[2] Though angular velocities fail to provide a proper choice of orientation coordinates, their nonintegrable nature provides greater control authority. It has been shown in recent years, for example, that complete reconfiguration of a rolling sphere in five dimensions is possible using only two angular velocities as control inputs.[3–5]

From our own research[5] on reconfiguration of the rolling sphere, it becomes clear that a certain sequence of rotations about axes confined to the horizontal plane is equivalent to a single rotation about the vertical axis. For the sequences proposed,[5] the point of contact between the sphere and the ground traces spherical triangles.[6,7] Though these results were obtained for a rolling sphere, they apply to general rigid body rotation. Also, closed curves on the sphere need not be restricted to spherical triangles; they can be lunes[8] or other spherical polygons.‡

The primary contribution of this Note lies in the use of spherical trigonometry for establishing a fundamental relationship in rotational kinematics, stated also by the Gauss–Bonet theorem[9] of parallel transport. The theorem essentially states that a rolling sphere, which depicts the rotational motion of a rigid body constrained to rotate about axes that are confined to one plane, undergoes a net change in orientation about the axis perpendicular to the plane when its point of contact traces a spherical polygon. The amount of rotation is equal to the solid angle enclosed by the polygon and the direction of rotation depends on the direction in which the polygon is traced. This result and its mathematical exposition reinforce the connection between spherical trigonometry and rotational kinematics, which has been pointed out in earlier works.[10] Apart from rotational kinematics, the result is also useful for other applications. For example, it helps us to us resolve the problem of image registration with space telescopes when they are pointed from one direction sequentially to other directions and back to the original direction, to generate an image of an extended region. The axis of the telescope traces out the edges of a spherical polygon on the infinite sphere when it is returned to its original pointing direction. To avoid the problem of image registration, one has to compensate for rotation of the telescope about its own axis, equal to the solid angle subtended by the traced spherical polygon.

Review of Spherical Trigonometry

A circle generated by a plane passing through the center of a sphere is a great circle. The angle on the sphere formed by intersecting arcs of two great circles is a spherical angle. The portion of the sphere bounded by arcs of three great circles is called a spherical triangle. Consider the spherical triangle in Fig. 1, whose vertices and spherical angles are P, Q, R and A, B, C, respectively. Let a, b, c denote the angles subtended by the arcs QR, RP, PQ at the center of the sphere. The important relations for the spherical triangle[6–8] are given by the law of sines,

$$\sin a/\sin A = \sin b/\sin B = \sin c/\sin C \tag{1}$$

the laws of cosines for sides,

$$\cos a = \cos b\cos c + \sin b\sin c\cos A \tag{2}$$

$$\cos b = \cos c\cos a + \sin c\sin a\cos B \tag{3}$$

$$\cos c = \cos a\cos b + \sin a\sin b\cos C \tag{4}$$

and the laws of cosines for angles,

$$\cos A = -\cos B\cos C + \sin B\sin C\cos a \tag{5}$$

$$\cos B = -\cos C\cos A + \sin C\sin A\cos b \tag{6}$$

$$\cos C = -\cos A\cos B + \sin A\sin B\cos c \tag{7}$$

Some useful relationships that can be derived[6–8] from the laws of cosines for sides are

$$\sin A\cos b = \sin C\cos B + \sin B\cos C\cos a \tag{8}$$

$$\sin B\cos c = \sin A\cos C + \sin C\cos A\cos b \tag{9}$$

$$\sin C\cos a = \sin B\cos A + \sin A\cos B\cos c \tag{10}$$

$$\sin a\cos C = \sin b\cos c - \sin c\cos b\cos A \tag{11}$$

$$\sin b\cos A = \sin c\cos a - \sin a\cos c\cos B \tag{12}$$

$$\sin c\cos B = \sin a\cos b - \sin b\cos a\cos C \tag{13}$$

$$\sin A\cos c = \sin B\cos C + \sin C\cos B\cos a \tag{14}$$

$$\sin B\cos a = \sin C\cos A + \sin A\cos C\cos b \tag{15}$$

$$\sin C\cos b = \sin A\cos B + \sin B\cos A\cos c \tag{16}$$

The area of a spherical triangle can be mathematically expressed as

$$\Delta = Er^2, \qquad E \triangleq (A + B + C - \pi) \tag{17}$$

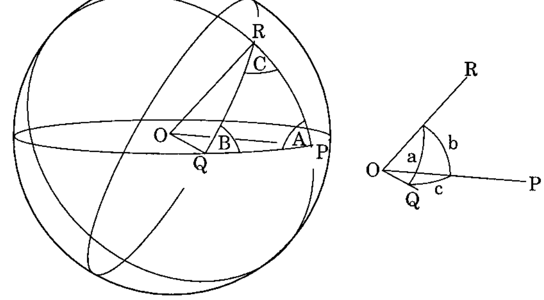

Fig. 1 Spherical triangle.

Received 12 July 1999; revision received 15 October 1999; accepted for publication 17 January 2000. Copyright © 2000 by the American Institute of Aeronautics and Astronautics, Inc. All rights reserved.

*Associate Professor, Department of Mechanical Engineering. 2555 Engineering Building; mukherji@egr.msu.edu.

†Graduate Student.

‡In the spirit of the common terminology "spherical triangle," we define a "spherical polygon" as a closed curve on the surface of a sphere comprised of multiple segments wherein each segment is an arc of a great circle.

where Δ is the area of the triangle, r is the radius of the sphere, and the spherical excess, E, is the solid angle subtended by the spherical triangle.

Rotation Induced by Spherical Triangles

Transformation Matrix

In this section we compute the rotation of the sphere in Fig. 1 when it rolls on the horizontal plane in a manner that its contact point traces a spherical triangle. Without any loss of generality, we assume the sphere to be initially located at the origin of the xyz frame in Fig. 2, with point Q in contact with the ground. To roll along the spherical triangle, the sphere is first rolled by angle a in the direction that brings the point of contact to R. Without loss of generality, let this direction be along the negative y axis. In the next step the sphere is rolled by angle b, in the direction oriented $(\pi - C)$ counterclockwise to the negative y axis. This brings the point of contact to P. Finally, the sphere rolls angle c in the direction oriented $(\pi - A)$ counterclockwise to the previous direction of rolling. This brings the contact point back to Q.

It is clear from Fig. 2 that the path traced by the sphere on the ground is not a closed path. However, the net translation of the sphere is not the subject of investigation here. We investigate the net rotation of the sphere, which is comprised of the sequential rotations 1) angle a about $\boldsymbol{i}$, 2) angle b about $[-\cos C\boldsymbol{i} + \sin C\boldsymbol{j}]$, and 3) angle c about $[\cos(A + C)\boldsymbol{i} - \sin(A + C)\boldsymbol{j}]$, where $\boldsymbol{i}, \boldsymbol{j}, \boldsymbol{k}$, are unit vectors along the x, y, z axes. By adopting the notation S_*, C_* to denote $\sin *$, $\cos *$, the transformation matrix representing the above sequence of rotations can be expressed as

$$\boldsymbol{R} \triangleq \begin{pmatrix} r_{11} & r_{12} & r_{13} \\ r_{21} & r_{22} & r_{23} \\ r_{31} & r_{32} & r_{33} \end{pmatrix} \tag{18}$$

where r_{ij}, $i = 1, 2, 3$, $j = 1, 2, 3$, after preliminary simplification, can be expressed as follows:

$$\begin{aligned} r_{11} &= C_c C_C^2 + C_b C_c S_C^2 + S_c C_C S_A S_b S_C + S_c C_A S_b S_C^2 \\ &\quad + (1 - C_c)(C_A C_C - S_A S_C)\big[C_C S_C^2 C_A - C_b C_C^2 S_C S_A \\ &\quad + C_C^3 C_A - C_b S_C^3 S_A\big] \end{aligned} \tag{19}$$

$$\begin{aligned} r_{12} &= -C_c C_C S_C + C_b C_c C_C S_C + S_c C_A C_C S_b S_C - S_c S_A S_b S_C^2 \\ &\quad - (1 - C_c)(C_C S_A + C_A S_C)\big[S_C^2 C_A C_C - C_b C_C^2 S_A S_C \\ &\quad + C_A C_C^3 - C_b S_C^3 S_A\big] \end{aligned} \tag{20}$$

$$r_{13} = -C_c S_b S_C + S_c\big[C_C S_A + C_A C_b S_C\big] \tag{21}$$

$$\begin{aligned} r_{21} &= S_c\big(-C_b C_C S_a S_A + C_a C_C^2 S_A S_b - C_A C_b S_a S_C \\ &\quad + C_a C_A C_C S_b S_C\big) + C_c[-C_a(1 - C_b)C_C S_C + S_a S_b S_C] \\ &\quad + (1 - C_c)(C_A C_C - S_A S_C)\big\{(C_A C_C - S_A S_C) \\ &\quad \times[-C_a(1 - C_b)C_C S_C + S_a S_b S_C] - (S_A C_C \\ &\quad + C_A S_C)\big[C_a C_b + S_a S_b C_C + C_a(1 - C_b)S_C^2\big]\big\} \end{aligned} \tag{22}$$

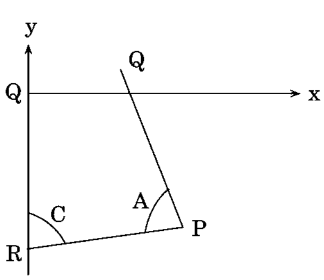

Fig. 2 Motion of the sphere in Fig. 1 generated by the spherical triangle *QRP*.

$$\begin{aligned} r_{22} &= S_c\big(-C_A C_b C_C S_a + C_a C_A C_C^2 S_b + C_b S_a S_A S_C \\ &\quad - C_a C_C S_A S_b S_C\big) + C_c\big[C_a C_b + C_C S_a S_b + C_a(1 - C_b)S_C^2\big] \\ &\quad - (1 - C_c)(C_A S_C + S_A C_C)\big\{(C_A C_C - S_A S_C) \\ &\quad \times[-C_a(1 - C_b)C_C S_C + S_a S_b S_C] - (S_A C_C + C_A S_C)\big[C_a C_b \\ &\quad + S_a S_b C_C + C_a(1 - C_b)S_C^2\big]\big\} \end{aligned} \tag{23}$$

$$\begin{aligned} r_{23} &= C_c(S_a C_b - C_a S_b C_C) + S_c[C_a C_b C_A C_C + S_a S_b C_A \\ &\quad - C_a S_A S_C] \end{aligned} \tag{24}$$

$$\begin{aligned} r_{31} &= S_c\big(-C_a C_b C_C S_A - S_a S_b C_C^2 S_A - C_a C_b C_A S_C \\ &\quad - S_a S_b C_A S_C C_C\big) + C_c[(1 - C_b)S_a S_C C_C + C_a S_b S_C] \\ &\quad + (1 - C_c)(C_A C_C - S_A S_C)\big\{(C_A C_C - S_A S_C) \\ &\quad \times[(1 - C_b)S_a S_C C_C + C_a S_b S_C] - (S_A C_C + C_A S_C)\big[-S_a C_b \\ &\quad + C_a S_b C_C - (1 - C_b)S_a S_C^2\big]\big\} \end{aligned} \tag{25}$$

$$\begin{aligned} r_{32} &= S_c\big(-C_a C_b C_A C_C - S_a S_b C_A C_C^2 + C_a C_b S_A S_C \\ &\quad + S_a S_b S_A S_C C_C\big) + C_c\big[-S_a C_b + C_a S_b C_C - (1 - C_b)S_a S_C^2\big] \\ &\quad - (1 - C_c)(S_A C_C + C_A S_C)\big\{(C_A C_C \\ &\quad - S_A S_C)\big[(1 - C_b)S_a S_C C_C + C_a S_b S_C) - (S_A C_C \\ &\quad + C_A S_C)(-S_a C_b + C_a S_b C_C - (1 - C_b)S_a S_C^2\big]\big\} \end{aligned} \tag{26}$$

$$\begin{aligned} r_{33} &= C_c(C_a C_b + S_a S_b C_C) + S_c(-S_a C_b C_A C_C + C_a S_b C_A \\ &\quad + S_a S_A S_C) \end{aligned} \tag{27}$$

Simplification Using Spherical Trigonometry

First, consider the term r_{13} in Eq. (21). It can be simplified using Eq. (9) as follows:

$$r_{13} = -C_c S_b S_C + S_c C_c S_B$$

Using Eq. (1) it can then be shown to be equal to zero,

$$r_{13} = -C_c S_b S_C + S_C C_c S_b = 0 \tag{28}$$

Next, consider the term r_{23} in Eq. (24). Use Eq. (13) to simplify the first two terms,

$$r_{23} = S_c[C_c C_B + C_a C_b C_A C_C + S_a S_b C_A - C_a S_A S_C]$$

Use Eqs. (6) and (4) to expand the first and second terms, respectively, and then simplify,

$$r_{23} = S_c S_C[C_c C_b S_A + S_a S_b C_A S_C - C_a S_A]$$

Expand the first term using Eq. (2) and cancel terms,

$$r_{23} = S_b S_c S_C C_A[-S_c S_A + S_a S_C]$$

Finally, use Eq. (1) to arrive at

$$r_{23} = S_b S_c S_C C_A[-S_C S_a + S_a S_C] = 0 \tag{29}$$

Since the rows and columns of $\boldsymbol{R}$ in Eq. (18) are orthonormal, it immediately follows that

$$r_{33} = 1.0, \qquad r_{31} = 0, \qquad r_{32} = 0 \tag{30}$$

From the values of $r_{13}, r_{23}, r_{31}, r_{32}, r_{33}$, it is clear that $\boldsymbol{R}$ in Eq. (18) is representative of a pure rotation about the z axis. To determine the amount of rotation, we first simplify the term r_{11} in Eq. (19). Using Eq. (6), we get

$$r_{11} = C_c C_C^2 + C_b C_c S_C^2 + S_c C_C S_A S_b S_C + S_c C_A S_b S_C^2 - C_B(1 - C_c)(C_A C_C - S_A S_C)$$

Expand using Eqs. (7) and (16),

$$r_{11} = C_c C_C^2 + C_b C_c S_C^2 + S_c C_C S_A S_b S_C + S_c C_A S_b S_C^2 - C_B C_A C_C + C_B S_A S_C + C_c C_C[S_A S_B C_c - C_C] - C_c S_C[S_C C_b - C_A S_B C_c]$$

Cancel terms and group the rest of the terms together,

$$r_{11} = S_b S_c S_C S_{(A+C)} - C_B C_{(A+C)} + C_c^2 S_B S_{(A+C)}$$

Use Eq. (1) to rewrite the first term. Simplification leads to the following final expression for r_{11},

$$r_{11} = S_B S_c^2 S_{(A+C)} - C_B C_{(A+C)} + C_c^2 S_B S_{(A+C)} = S_B S_{(A+C)} - C_B C_{(A+C)} = -C_{(A+B+C)} \tag{31}$$

Using Eqs. (2) and (6), the term r_{12} in Eq. (20) can be simplified to

$$r_{12} = -C_c C_C S_C + C_a C_C S_C - S_c S_A S_b S_C^2 + C_B(1 - C_c)(C_C S_A + C_A S_C)$$

Expand the terms in parentheses,

$$r_{12} = -C_c C_C S_C + C_a C_C S_C - S_c S_A S_b S_C^2 + C_B C_C S_A + C_B C_A S_C - C_c C_B C_C S_A - C_c C_B C_A S_C$$

Group the first and last terms using Eq. (7) and expand the second term using Eq. (10),

$$r_{12} = -C_c^2 S_C S_A S_B + C_C C_A S_B - S_c S_A S_b S_C^2 + C_B C_C S_A + C_B C_A S_C$$

Group the second and last terms and use Eq. (1) to rewrite the third term. On simplification, r_{12} takes the final form,

$$r_{12} = -C_c^2 S_C S_A S_B + C_A S_{(B+C)} - S_c^2 S_A S_B S_C + C_B C_C S_A = C_A S_{(B+C)} - S_A S_B S_C + C_B C_C S_A = S_{(A+B+C)} \tag{32}$$

Using the orthonormal property of the rows of $\boldsymbol{R}$, the remaining entries can be argued to be

$$r_{21} = -S_{(A+B+C)}, \qquad r_{22} = -C_{(A+B+C)} \tag{33}$$

The above simplifications establish that the rotation matrix in Eq. (18) has the form

$$\boldsymbol{R} = \begin{pmatrix} -C_{(A+B+C)} & S_{(A+B+C)} & 0 \\ -S_{(A+B+C)} & -C_{(A+B+C)} & 0 \\ 0 & 0 & 1 \end{pmatrix} = \begin{pmatrix} C_E & -S_E & 0 \\ S_E & C_E & 0 \\ 0 & 0 & 1 \end{pmatrix} \tag{34}$$

where E, defined in Eq. (17), is the solid angle subtended by the spherical triangle. As mentioned earlier, the matrix in Eq. (34) corresponds to pure rotation about the vertical axis. This is not surprising since the point on the sphere in contact with the ground before rolling is the same as that after rolling. Also, the direction of rotation, for the path considered in Fig. 2, is along the negative z axis. The path in Fig. 2 is left-handed since the sphere always turns left, as viewed by an observer inside the sphere. It can be shown that the sphere rotates about the positive z axis for right-handed paths and about the negative z axis for left-handed paths.

Generalization to Spherical Polygons

In this section we first show that the results obtained in the previous section apply to lunes.[8] A lune, shown in Fig. 3, is a closed

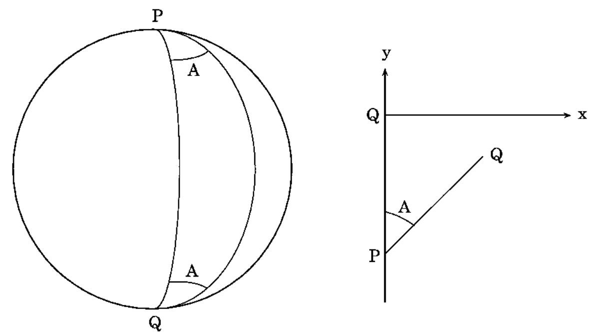

Fig. 3 Lune and its image on the ground.

curve generated by arcs of two great circles. The two angles of intersection of the arcs, which are necessarily equal, are denoted A. The length of the arcs are also the same and equal to half the circumference of the great circle. As in the previous section, we assume that the sphere is initially at the origin with point Q in contact with the ground. It rolls angle π about the x axis to bring point P in contact with the ground. Subsequently, it changes direction $(\pi - A)$ counterclockwise and rolls angle π. At the end of this motion, point Q is again in contact with the ground. The net rotation of the sphere can be described by the rotation matrix

$$\boldsymbol{R} = \begin{pmatrix} C_{2A} & -S_{2A} & 0 \\ S_{2A} & C_{2A} & 0 \\ 0 & 0 & 1 \end{pmatrix} \tag{35}$$

which is equivalent to a rotation by angle $2A$ about the negative z axis. Indeed, the solid angle subtended by the lune is $2A$, and the path traced by the sphere is left-handed.

The results in the previous section can be extended to spherical polygons by showing that an arbitrary polygon can be generated by a combination of lunes and spherical triangles. The net rotation of the sphere, as it traces the spherical polygon, can be expressed as the sum of the rotations due to the individual lunes and triangles. Of course, the rotation associated with each lune and triangle will be positive, or negative, depending upon whether the path is right-handed, or left-handed.

Conclusion

We use spherical trigonometry to prove the Gauss–Bonet theorem,[9] which states essentially that the net rotation of a sphere rolling along a closed path on its surface, comprised of arcs of great circles, equals the solid angle subtended by the path. The mathematical exposition of this result strengthens the connection between rotational kinematics and spherical trigonometry.

Acknowledgment

The authors gratefully acknowledge the support provided by the National Science Foundation, NSF Grant CMS-9800343, in carrying out this research.

References

[1]Junkins, J. L., and Turner, J. D., *Optimal Spacecraft Rotational Maneuvers*, Elsevier, New York, 1986, Chaps. 1 and 2.

[2]Greenwood, D. T., *Principles of Dynamics*, Prentice–Hall, Englewood Cliffs, NJ, 1988, p. 450.

[3]Li, Z., and Canny, J., "Motion of Two Rigid Bodies with Rolling Constraints," *IEEE Transactions on Robotics and Automation*, Vol. 6, No. 1, 1990, pp. 62–72.

[4]Jurdjevic, V., "The Geometry of the Plate-Ball Problem," *Archives for Rational Mechanics and Analysis*, Vol. 124, No. 4, 1993, pp. 305–328.

[5]Mukherjee, R., Minor, M., and Pukrushpan, J. T., "Simple Motion Planning Strategies for Spherobot: A Spherical Mobile Robot," Proceedings of 38th IEEE International Conf. on Decision and Control, Phoenix, AZ, 1999.

[6]Kells, L. M., Kern, W. F., and Bland, J. R., *Plane and Spherical Trigonometry*, McGraw–Hill, New York, 1940, pp. 289–293.

[7]Ayres, Jr., F., *Schaum's Outline of Theory and Problems of Plane and Spherical Trigonometry*, McGraw–Hill, New York, 1954.

[8]Todhunter, I., *Spherical Trigonometry*, 4th ed., Macmillan, London, 1878.

[9]Levi, M., "Geometric Phases in the Motion of Rigid Bodies," *Archives for Rational Mechanics and Analysis*, Vol. 122, No. 3, 1993, pp. 213–229.
[10]Junkins, J. L., and Shuster, M. D., "The Geometry of Euler Angles," *Journal of the Astronautical Sciences*, Vol. 41, No. 4, 1993, pp. 531–543.

Finite Element and Runge–Kutta Methods for Boundary-Value and Optimal Control Problems

Carlo L. Bottasso* and Andrea Ragazzi†
Politecnico di Milano, 20158 Milan, Italy

Introduction

WE consider a class of finite element in time (FET) and some implicit Runge–Kutta (RK) schemes for the solution of boundary-value problems. FETs have been recently advocated as a new way of solving this class of problems, with particular emphasis on optimal control problems (for example, see Ref. 1 and the references therein). The finite element method develops solutions discretizing appropriate weak forms of the equations that describe a given problem. On the other hand, the RK method directly discretizes the governing ordinary differential equations (ODEs). Although the two approaches look different, in this work we prove that the discrete equations arising from the class of FETs here considered are linear combinations of the equations generated by some implicit RK schemes and that the FET unknowns are linear combinations of the RK unknowns within each time step. Under these circumstances, this means that the two approaches are in reality the same method that yields identical numerical solutions and, hence, enjoys the same numerical properties. The analysis is valid for the p version of the method, that is, for arbitrarily high order. Similar results were derived in Ref. 2 for initial-value problems. That work is here extended to cover the case of boundary-value differential-algebraic problems.

RK methods are probably the best understood and most widely studied family of integration schemes, which makes them a mature and trusted technology with extensive applications to the class of problems here considered. FETs are less widely known, but their application to certain problems leads to strikingly simple solution procedures, for example, in the case of optimal control.[3] Our hope is that the proof of equivalence here offered might help close the gulf existing between practitioners using the two methods. We believe that additional insight can be usually obtained by a unified view, and we are, therefore, not suggesting to abandon one approach in favor of the other. Furthermore, some developments, for example a posteriori error estimation for adaptive mesh control, might be easier to accomplish in one framework rather than in the other.[4]

Boundary-Value Problems

We consider a generic boundary-value problem, defined by a system of first-order ODEs

$$\dot{\boldsymbol{y}} = \boldsymbol{g}(\boldsymbol{y}, z, t) \tag{1a}$$

If algebraic constraints of the form

$$\boldsymbol{a}(\boldsymbol{y}, z, t) = 0 \tag{1b}$$

are also present, we have an index-one differential-algebraic equation (DAE) problem. In Eqs. (1a) and (1b), $(\dot{\cdot}) = \mathrm{d}\cdot/\mathrm{d}t$, $\boldsymbol{y} \in \mathbb{R}^Y$, $z \in \mathbb{R}^Z$, $t \in \mathbb{R}$, $\boldsymbol{g}: \mathbb{R}^Y \times \mathbb{R}^Z \times \mathbb{R} \to \mathbb{R}^Y$, and $\boldsymbol{a}: \mathbb{R}^Y \times \mathbb{R}^Z \times \mathbb{R} \to \mathbb{R}^Z$. $I = [0, T]$ is the time domain. Suitable boundary and additional constraint conditions are given as

$$\boldsymbol{C}[\boldsymbol{y}(0), \boldsymbol{y}(T), T] = 0 \tag{1c}$$

This format covers a wide range of applications, in particular optimal control problems with or without unknown terminal time and path constraints. Minor modifications allow treatment of problems with interior point constraints, possibly at unknown intermediate times, and multiphase problems (see Ref. 4 and references therein for details).

We partition I according to $0 = t_1 < t_2 < \cdots < t_{N+1} = T$ and let $h_n := t_{n+1} - t_n$. We consider global methods, that is, methods that produce an approximate solution representation over the entire interval of interest. In the terminology of the finite element method, these procedures assemble the equations over the whole interval. Alternative strategies are based on the solution of corresponding initial-value problems, for example, shooting and related techniques.

RK Methods

The ε-embedding method[5] for an s-stage RK scheme applied to the solution of Eqs. (1a) and (1b) results in the relations

$$\hat{\boldsymbol{y}} = (\boldsymbol{1} \otimes \mathbb{I}_Y)\boldsymbol{y}^n + h_n(\boldsymbol{A} \otimes \mathbb{I}_Y)\hat{\boldsymbol{g}} \tag{2a}$$

$$0 = \hat{\boldsymbol{a}} \tag{2b}$$

$$\boldsymbol{y}^{n+1} = \boldsymbol{y}^n + h_n(\boldsymbol{b}^T \otimes \mathbb{I}_Y)\hat{\boldsymbol{g}} \tag{2c}$$

where $\boldsymbol{b}, \boldsymbol{c} \in \mathbb{R}^s$ and $\boldsymbol{A}$ is $s \times s$. The sY-dimensional vectors are defined as $\hat{\boldsymbol{y}} := (\boldsymbol{y}^1, \ldots, \boldsymbol{y}^s)$ and $\hat{\boldsymbol{g}} := [\boldsymbol{g}(\boldsymbol{y}^1, z^1, t^1), \ldots, \boldsymbol{g}(\boldsymbol{y}^s, z^s, t^s)]$ and the sZ-dimensional vectors as $\hat{z} := (z^1, \ldots, z^s)$ and $\hat{\boldsymbol{a}} := [\boldsymbol{a}(\boldsymbol{y}^1, z^1, t^1), \ldots, \boldsymbol{a}(\boldsymbol{y}^s, z^s, t^s)]$, where $t^i := t_n + c_i h_n$. Finally, the symbol $\otimes$ denotes the tensor (Kronecker) product of matrices, whereas $\boldsymbol{1}$ is the s-dimensional vector $\boldsymbol{1} := (1, \ldots, 1)$ and $\mathbb{I}_Y$ is the unit $Y \times Y$ matrix.

Equations (1c) do not require discretization and, therefore, can be dropped from the subsequent discussion. The values $z^1, z^2, \ldots, z^{N+1}$ can be computed a posteriori, using the equations $\boldsymbol{a}(\boldsymbol{y}^{n+1}, z^{n+1}, t_{n+1}) = 0$, so that the solution $(\boldsymbol{y}^{n+1}, z^{n+1})$ lies on the manifold.

FET Methods

FET methods are based on the approximation of a weak form of Eqs. (1a–1c):

$$\int_I [\boldsymbol{v} \cdot (\dot{\boldsymbol{y}} - \boldsymbol{g}) + \boldsymbol{w} \cdot \boldsymbol{a}]\,\mathrm{d}t + \boldsymbol{\theta} \cdot \boldsymbol{C} = 0 \tag{3}$$

In practice, one seeks a solution that satisfies in a weak sense Eqs. (1a) and (1b) and the boundary conditions (1c). See Refs. 2 and 6 for a unified approach to FETs and the references cited in 4 for additional background and information. Integration by parts of the first term of Eq. (3) yields

$$\int_I (\dot{\boldsymbol{v}} \cdot \boldsymbol{y} + \boldsymbol{v} \cdot \boldsymbol{g} - \boldsymbol{w} \cdot \boldsymbol{a})\,\mathrm{d}t = \boldsymbol{v} \cdot \boldsymbol{y}|_{\partial I} + \boldsymbol{\theta} \cdot \boldsymbol{C} \tag{4}$$

Under certain circumstances, weak forms (3) and (4) can be given a variational interpretation (for example, see Ref. 2). This is also the point of view of Ref. 3.

The approximation of Eq. (4) is developed as follows. We construct finite-dimensional trial function spaces Y^h and Z^h as $Y^h := \{\boldsymbol{y}^h \in [\mathcal{P}^{k_y}(I_n)]^Y\}$ and $Z^h := \{z^h \in [\mathcal{P}^{k_z}(I_n)]^Z\}$, and test function spaces V^h and W^h as $V^h := \{\boldsymbol{v}^h \in [\mathcal{P}^{k_v}(I_n)]^Y\}$ and $W^h := \{\boldsymbol{w}^h \in [\mathcal{P}^{k_w}(I_n)]^Z\}$. $\mathcal{P}^k$ denotes the space of the kth-order polynomials. Within the nth time element, the finite element trial solutions are defined as follows:

$$\boldsymbol{y}^h(t) := \boldsymbol{y}^n$$

for $\tau = 0$,

$$\boldsymbol{y}^h(t) := \sum_{i=1}^{k_y+1} s_i^{k_y}(\tau)\boldsymbol{y}_i$$

Received 21 June 1999; revision received 30 March 2000; accepted for publication 2 April 2000.

*Ricercatore, Dipartimento di Ingegneria Aerospaziale, Via La Masa 34; Carlo.Bottasso@polimi.it.
†Graduate Student, Dipartimento di Ingegneria Aerospaziale, Via La Masa 34.